Molecular Vision 2024; 30:229-238 <http://www.molvis.org/molvis/v30/229>
Received 19 May 2022 | Accepted 20 April 2024 | Published 22 April 2024

Assessment of anterior scleral thickness in myopes and emmetropes using anterior segment optical coherence tomography

Zhi-liang Li,[1] Qi Xiong,[2] Shun-cheng Cai,[2] Yue Fu,[2] Yu-ting Li,[2] Xiao-min Chen,[2] Lin Yang,[2] Min Ke[2]

(The first three authors contributed equally to this work.)

[1]Department of Orthopedics, Renmin Hospital of Wuhan University, Wuhan, China. ; [2]Department of Ophthalmology, Zhongshan Hospital of Wuhan University, Wuhan, China

Purpose: To investigate the differences in anterior scleral thickness (AST) among the refractive statuses of Chinese adults aged 18–35.

Methods: This study recruited 170 Chinese participants (mean age, 24.06 ± 2.78 years), including myopes (spherical equivalent refraction [SER] –1.00 to –12.75 diopters [D]; n = 134), emmetropes (SER ± 0.75 D; n = 36), and AST (superior, inferior, nasal, and temporal), which were investigated via swept-source optical coherence tomography. Semiautomated custom-designed software measured the scleral thickness from the scleral spur to 5 mm along four meridians.

Results: The mean axial length and spherical equivalent refractive error were 25.12 ± 1.44 mm and −3.93 ± 3.09 D, respectively. The anterior sclera was thickest in the inferior region and thinnest in the superior region (753.9 ± 88.7 µm versus 613.6 ± 58.4; $p < 0.001$). The AST in the temporal meridian was significantly thicker than that in the nasal meridian (727.5 ± 60.8, 690.9 ± 55 µm; $p < 0.001$). There were no significant variations in AST in the myopes and emmetropes along the five latitude lines. AST along the inferior meridian at the 4-mm ($r 2 = 0.0992$; $p < 0.001$) and 5-mm ($r 2 = 0.0888$; $p < 0.001$) locations decreased significantly with increasing myopia.

Conclusion: With increased myopia, AST at the 4-mm and 5-mm locations showed significant thinning in the inferior meridian. The results indicate that AST, especially along the inferior meridian, may act as a biologic marker to monitor the progression of myopia.

Myopia currently affects approximately 30% of the world's population. By 2050, myopia will affect up to 50% of the Earth's population. Accordingly, it is progressively becoming a public health concern worldwide [1]. Eyes with myopia, especially high myopia characterized by longer axial lengths, are likelier to enable pathologic changes such as myopic maculopathy, retinal detachment, myopic choroidal neovascularization, and myopic optic neuropathy. These diseases are closely associated with exacerbated myopia [2,3]. Although the underlying pathogenesis of myopia remains elusive, numerous studies have indicated the significant role of the sclera (particularly at the posterior pole) in the development of myopia. The sclera is a fibrillar viscoelastic tissue that plays an important role in ocular shape and size. It has been reported that with the development of myopia, the sclera undergoes remodeling and thinning [4,5]. In animal studies, posterior segment scleral thinning and changes in collagen fiber diameter and organization have been found in the development of myopia [5,6]. As in all species examined, numerous studies have indicated that the posterior segment sclera becomes thinner according to the degree of myopia in humans [7,8].

The introduction of anterior segment optical coherence tomography (AS-OCT), especially swept-source anterior segment optical coherence tomography (SS-AS-OCT), has allowed us to observe cross-sectional images of the anterior sclera and measure its thickness in vivo. SS-AS-OCT has a higher penetration capacity of light signals, providing excellent repeatability and reliable measurement results. Researchers have begun to investigate the anterior scleral structure and thickness in myopia [9–11]. However, regional variations in the anterior and posterior segments have not been investigated, and disparate longitudinal studies have drawn disparate conclusions. Pekel et al. observed no significant differences between high myopia and emmetropic healthy controls in a cross-sectional comparative study [11,12]. Buckhurst and Read found that anterior scleral thickness (AST) was significantly greater in men, while no significant variations were found in refractive error or ethnicity [12]. Interestingly, Dhakal et al. found that with greater myopia, the anterior scleral thickness became thinner in the inferior meridian than in the other three (superior, nasal, and temporal) meridians [13]. The controversial results may be due to racial differences, selection bias resulting from the sectionalization of refractive error, age range differences, and

Correspondence to: Min Ke Department of Ophthalmology Zhongnan Hospital of Wuhan University No.169 Donghu Road, Wuchang District Wuhan, Hubei, 430071, China; Phone: +8618672395959; FAX: 027-67812622; email: keminyk@163.com

aspects of the chosen meridians (nasotemporal or temporal meridians only). In addition, the resolution of the instruments might have contributed to these divergent findings. The higher the resolution and deeper the scan of the instruments, the more precise the measurement. The second-generation SS-AS-OCT (CASIA 2; TOMEY), with the wavelength centered on 1,310 nm and 50,000 A-scans per second scan rate, can reach a maximum depth of 13 mm, which is much more powerful than the first generation [14]. In our study, we aimed to investigate the anterior scleral thickness across meridians (i.e., superior, inferior, nasal, and temporal) and five latitude lines (i.e., SNIT1, SNIT2, SNIT3, SNIT4, and SNIT5) in emmetropes and different degrees of myopia using new-generation SS AS OCT.

METHODS

Participants: In this study, 176 participants aged 18–35 years (mean 24.06 ± 2.78 years) were recruited randomly between June 2021 and November 2021 at Wuhan University's Zhongnan Hospital. All subjects signed written informed consent forms. The exclusion criteria included a history or evidence of systemic or ocular disease, injury, or surgery. Finally, six participants were excluded due to image quality, and 170 people were included in the study. The study's protocol was performed according to the tenets of the Declaration of Helsinki and was approved by the Ethics Committee of Zhongnan Hospital of Wuhan University (No. LYL2022010).

Each participant's objective refraction (ARK-1a; NIDEK, Gamagori, Japan) and best-corrected visual acuity (BCVA) were determined to ensure that all participants had a best-corrected visual acuity of at least logMAR 0.00. Subsequently, the spherical equivalent refractive (SER) error was obtained via noncycloplegic subjective refraction, and subjects were categorized as emmetropes (SER + 0.75 to –0.75 D; age, 24.36 ± 3.51 years; n = 36), low myopia (SER ≤ –1.00 to –3.00 D; age, 24.05 ± 2.31 years; n = 40), moderate myopia (SER ≤ –3.25 to –6.00 D; age, 23.87 ± 2.44 years; n = 54), and high myopia (SER ≤ –6.25 D; age, 24.08 ± 2.98 years; n = 40). There was no significant age distinction between these groups. Detailed ophthalmic examinations were conducted, including fundus examination, slit-lamp biomicroscopy, axial length, wide-angle fundus photography, AS-OCT, and spectral domain optical coherence tomography (SD-OCT). Axial length measurements were taken with an IOL Master 700 (Carl Zeiss Meditec, La Jolla, CA), and wide-angle fundus photography was performed with an Optos Daytona Ultrawide field fundus camera (SLO; Optos, Daytona, UK). Subfoveal choroidal thickness (SFCT) was measured using SD-OCT (HRA + OCT Spectralis, Heidelberg Engineering, Heidelberg, Germany). AST was measured using second-generation SS AS OCT (CASIA 2; TOMEY).

Image acquisition: Scleral cross-sectional images were acquired using SS-AS-OCT. Before the examination, four fixed superior, inferior, nasal, and temporal location markers were placed externally, and the correct head position of each patient was ensured. All subjects were asked to focus on the four fixed locations external to the instrument, while the imaging plane angle was altered to match the meridian during the scan. The raster scan protocol (16 B-scans with a width of 4 mm) was performed to obtain AST information. The scan line along the horizontal and vertical meridians (temporal, nasal, superior, and inferior) passed accurately through the central cornea to ensure consistency in obtaining AST. Simultaneously, the subject gazed fixedly at a suitably located target for approximately five seconds (Figure 1). The raster scan was performed in the same region for all repeated image acquisitions. Only quality images (signal ≥ 50% of maximum strength, without imaging distortions or artifacts) were adopted. SFCT was performed using SD-OCT. A horizontal B-scan running through the fovea was conducted in enhanced depth imaging (EDI) mode to obtain high-resolution OCT images. All examinations were performed by two skilled operators at 10–12 AM to avoid potential diurnal variations in ocular parameters.

Image analysis: Only data from the right eye were selected for statistical analysis. The thickness profile from the central line was extracted and analyzed to ensure the same anterior eye region. The scleral thickness was measured manually using preinstalled OCT software. The scleral thickness was defined as the vertical distance between the outer and inner scleral boundaries on the B-scan images. Following previous studies using AS-OCT to measure AST, we defined the deep episcleral blood vessel plexus, which presents as a low reflectivity region in the scan, as the outer boundary [10,11,13,15,16]. The inner boundary is a distinct demarcation between scleral tissue with high reflectivity and ciliary–choroid body tissue. The position of the scleral spur, according to a previously defined standard, was a slight protrusion of the sclera into the anterior chamber [13]. The scleral thickness was measured vertically from the scleral spur to discrete points of 1 mm, 2 mm, 3 mm, 4 mm, and 5 mm on the outer boundary in four meridians (superior, inferior, nasal, and temporal) separately (the method used by Imanaga et al.) [17] (Figure 2). Due to extraocular muscle insertion at locations approximately 6 mm posterior to the scleral spur, measurements beyond 5 mm were excluded from the analyses. The vertical distance between the outer border of the retinal pigment epithelium (RPE) and the inner

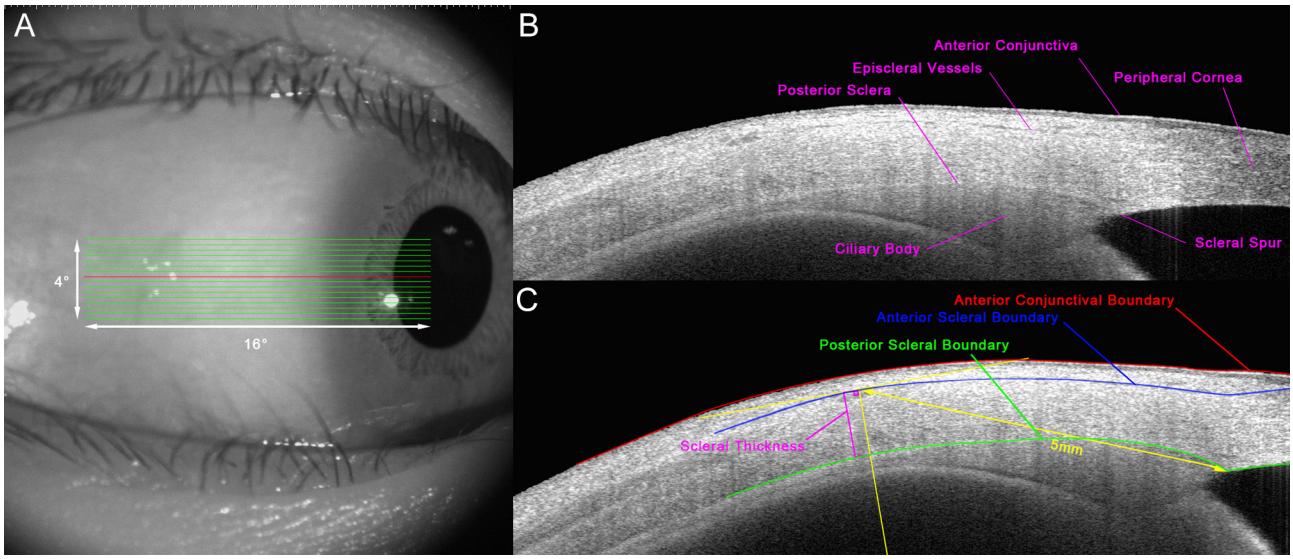

Figure 1. AS-OCT images.s **A**: AS-OCT image of the anterior scleral scanning protocol. A 16° × 4° volume B-scan with 21 lines was conducted to obtain images of the anterior temporal sclera. **B**: A B-scan of the anterior temporal sclera with anatomic landmarks labeled. **C**: A B-scan with semi-automated segmentation, delineating the anterior scleral boundary (marked in blue), the posterior scleral boundary (marked in green), the anterior conjunctiva boundary (marked in red), and the scleral thickness (marked in amaranth).

border of the posterior sclera at the fovea was defined as the subfoveal choroidal thickness. OCT images with insufficient quality (a signal strength < 70) or in cases where the interface of RPE and chorioscleral were not distinctly distinguished were eliminated from the analysis. All measurements were made manually by one experienced technician, for whom the subjects' basic information was masked. Twenty anterior scleral images were selected randomly to evaluate interobserver and intraobserver variability in AST. For intraobserver variability, the observer (CSC) measured the same images one week after the initial measurements. To determine interobserver variability, the same images were measured independently by two observers (XQ and CSC).

Statistical analysis: IBM SPSS Statistics 22.0 (IBM Corp., Armonk, NY) was used to conduct the statistical analysis, and MS Excel 2018 (Microsoft Corporation) was applied to plot the graphs. The Shapiro–Wilk test was used to assess whether the average AST along the four meridians and five latitude lines was normally distributed. Four (superior, inferior, nasal, and temporal) repeated-measures ANOVA with the Bonferroni post-hoc test were performed separately. Similarly, repeated-measures ANOVAs were performed to evaluate five latitude lines (i.e., SNIT1, SNIT2, SNIT3, SNIT4, and SNIT5). The Dunnett method was used to adjust p-values involving a post-hoc test. To investigate whether the AST slopes in each of the four meridians and five latitude lines

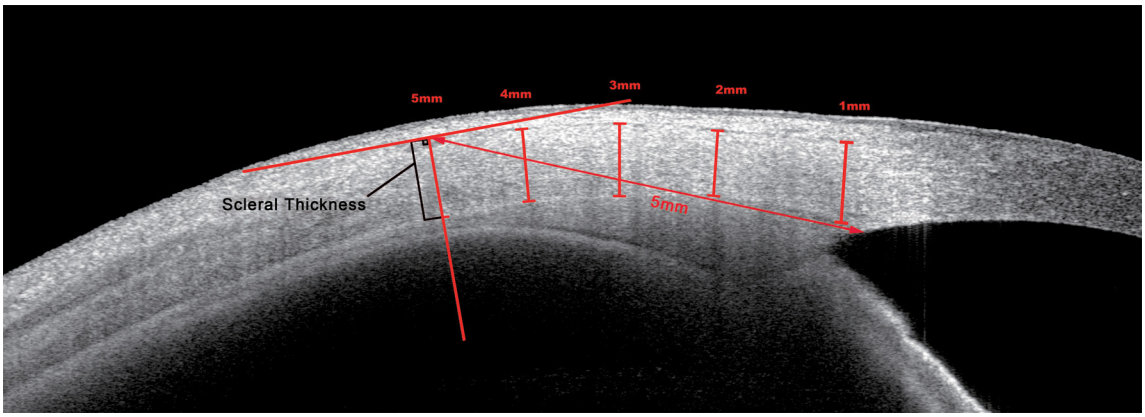

Figure 2. Measurement protocol of scleral thickness. The scleral thickness is measured vertically 1–5 mm posterior to the scleral spur.

were significantly different, a linear regression analysis was performed according to SER error. Pearson correlation analysis was used to analyze the correlation between axial length and scleral thickness in the superior, inferior, nasal, and temporal directions. P values < 0.05 were considered statistically significant.

RESULTS

A total of 170 adults with a mean age of 24.06 ± 2.78 years (range 18–35 years) were enrolled. The mean axial length and SER error were 25.12 ± 1.44 mm and −3.93 ± 3.09 D, respectively. The mean SFCT values were 341.74 ± 15.25 µm (emmetropes), 312.69 ± 14.66 µm (low myopic), 236.24 ± 9.06 µm (moderate myopic), and 204.97 ± 11.84 µm (high myopic; Table 1). The tests of interobserver and intraobserver variation both showed good repeatability of the AST measurements (ICC ≥ 0.98 and ICC ≥ 0.976, respectively). The CV was <9.4% for all AST parameters (Table 2).

The average thickness profile of the sclera along four meridians and five latitude lines is illustrated in Table 3. Repeated measures ANOVA showed that the AST varied significantly along the four meridians and the five latitude lines ($p < 0.001$). The AST was thinner in the nasal meridian than in the temporal meridian (690.9 ± 55 versus 727.5 ± 60.8 µm; $p < 0.001$), but thinner in the superior meridian than in the inferior meridian (613.6 ± 58.4 versus 753.9 ± 88.7 µm; $p < 0.001$). The average AST was thickest at the 1-mm latitude line (SNIT1: 719.2 ± 59.6 µm) and thinnest at the 5-mm latitude line (SNIT5: 688.6 ± 60.9 µm). The average AST was thickest at the 3-mm latitude lines (SNIT3: 720.4 ± 50.8 µm) in emmetropes and thickest at 1 mm latitude lines in myopes (SNIT1: 720.1 ± 58.6 µm).

Significant differences in the averaged AST were found to be associated with myopia along the inferior meridian ($p < 0.001$; Table 4). At i4, the mean scleral thickness in the orthopeadic group was higher than that in the severe myopia group ($p = 0.006$, adjusted by DUNNETT), and the same trend was observed at i5 ($p = 0.0031$, adjusted by DUNNETT; Figure 3). Linear regression analysis was further performed between the inferior meridian and the degree of refractive error, revealing significant scleral thinning with increasing degrees of myopia only at 4-mm ($r 2 = 0.0992$; $p < 0.001$) and 5-mm ($r 2 = 0.0888$; $p < 0.001$) locations from the limbus, and the maximum changes were at the 5-mm locations (Figure 4). The AST along the five latitude lines revealed no significant distinctions in myopes and emmetropes. In addition, there was no correlation between axial length and scleral thickness in the superior, inferior, nasal, and temporal directions (Appendix 3).

DISCUSSION

This study is the first to investigate AST in vivo along four meridians and five latitude lines in emmetropia and myopia using SS AS-OCT in young Chinese adults. Both the interobserver and intraobserver reliability of AST measurements was good. Our study provides quantitative evidence of asymmetric scleral thickness both along the vertical meridian (inferior AST thicker than superior) and along the horizontal meridian (temporal AST thicker than nasal). The average AST is thickest at 1-mm latitude lines and thinnest at 5-mm latitude lines. Moreover, with increased myopia, the AST was significantly reduced at the 4-mm and 5-mm locations along the inferior meridian.

Table 1. Demographic and ocular characteristics of the study participants.

Variables		Mean±SD
Ages (years)		24.06±2.78
Axial length (mm)		25.12±1.44
SEM refractive error (D)		−3.93±3.09
	Emmetropes	−0.15±0.33
	Low myopic	−2.16±0.70
	Moderate myopic	−4.46±0.76
	High myopic	−8.37±1.72
Subfoveal CT (µm)		271.58±95.29
Emmetropes		341.74±15.25
Low myopic		312.69±14.66
Moderate myopic		236.24±9.06
High myopic		204.97±11.84

SE, spherical equivalent; CT, choroid thickness.

Table 2. Reproducibility of AST measurements (n=20 subjects) at 1–5 mm from the scleral spur.

Intra-observer	Session	Mean ± SD	CV	ICC (95% CI)
AST1	Session 1	818.7±66.8	8.07%	0.988 (0.969–0.996)
	Session 2	820.7±67.5		
AST2	Session 1	790.5±63.5	8.29%	0.98 (0.949–0.992)
	Session 2	793.7±65.7		
AST3	Session 1	811.6±71.1	8.62%	0.989 (0.971–0.995)
	Session 2	807.9±70.4		
AST4	Session 1	812.6±53.9	6.67%	0.981 (0.953–0.992)
	Session 2	809.2±55.6		
AST5	Session 1	784.7±73.3	9.31%	0.989 (0.973–0.996)
	Session 2	787.1±75		
Inter-observer		Mean ± SD	CV	ICC (95% CI)
AST1	Observer 1	818.7±66.8	8.67%	0.987 (0.967–0.995)
	Observer 2	826±72		
AST2	Observer 1	790.5±63.5	8.45%	0.986 (0.965–0.994)
	Observer 2	796.7±67.3		
AST3	Observer 1	811.6±71.1	8.84%	0.99 (0.976–0.996)
	Observer 2	816.5±72.2		
AST4	Observer 1	812.6±53.9	6.38%	0.979 (0.948–0.992)
	Observer 2	807.2±50.5		
AST5	Observer 1	784.2±73.2	9.29%	0.976 (0.938–0.991)
	Observer 2	790.7±74.9		

SD=standard deviation; CV=coefficient of variation; ICC=intraclass correlation coefficient; 95% CI=95% confidence interval.

Numerous studies have demonstrated consistent results that the AST is thickest at the scleral spur [4,11,18,19]. Moreover, the AST was measured vertically from the scleral spur to the 1-, 2-, 3-, 4-, and 5-mm locations (Figure 2). The location at 1 mm approached the scleral spur. Consequently, the AST at the scleral spur was not included in the current study. The sclera was thickest in the inferior meridian and thinnest in the superior meridian. Similar results were reported by Norman et al., who used a three-dimensional MRI to investigate the scleral thickness of 11 enucleated eyes [19]. Buckhurst et al. and Dhakal et al. used AS-OCT to measure AST along the horizontal and vertical meridians in Caucasians and Indians, which corroborates our results [9,13]. The AST along each meridian varies in diverse studies. Read et al. [11] (included ≤ -8.00 D) and Dhakal et al. [13] (included ≤ -27.25 D) both showed thinner AST (thinner by >100 µm) compared with our study. Thus, the range of myopia may not be the reason for such differences in scleral thickness, and other factors, such as the role of ethnicity in myopia, may play a role. Disparities in eye shape have been identified among different ethnicities. Oliveira et al. reported that the temporal scleral thickness was thinner in Caucasians than in non-Caucasians [20].

Table 3. A ST for four meridians (superior (S), inferior (I), nasal (N), temporal (T)) and five latitude lines (SINT1, SINT2, SINT3, SINT4, SINT5) and distance (1–5 mm) from the SS (mean ± SD mm).

Meridians	AST at distances from SS (mm)					Average
	1	2	3	4	5	
Superior	628.5±61.5	625.6±54.4	625.6±58.1	601.6±73.7	586.7±91.4	613.6±58.4
Inferior	810.6±76.9	788.9±65.7	803.4±70.4	779.7±70.9	755.2±89.4	753.9±88.7
Temporal	751.6±88	699.7±66	741.5±70.6	753.3±71.4	739.5±87.5	727.5±60.8
Nasal	694.2±73.5	698.7±58.5	705.9±60.3	687.4±68.4	677.2±78.7	690.9±55
Average	719.2±59.6	703.1±52.1	719±52.9	705.3±52.1	688.6±60.9	706.4±97.7

Table 4. AST with different SER error along four meridians (superior-S, inferior-I, nasal-N, temporal-T).

Meridians	Thickness	Emmetropes	Low myopic	Moderate myopic	High myopic	P value
Superior	1 mm	623.3±68.7	620.5±46.4	631.7±64.9	637±64.1	0.42491
	2 mm	621.5±58.1	626.1±51.8	619.8±50.4	636.6±58.9	
	3 mm	617.6±56.7	623.3±51.7	616.3±53.7	647.7±67	
	4 mm	598±66.5	600.5±75.7	593±62.5	617.5±90.2	
	5 mm	599.9±89.6	573.5±86.9	581±81.3	595.4±109.5	
Inferior	1 mm	807.9±72	805.9±72.9	810.2±794.5	818±84.1	<0.0001
	2 mm	794±61.6	788.7±61.5	785.1±69	789.6±70.4	
	3 mm	819.9±59.5	801.1±80.4	796.3±66.7	800.4±73.8	
	4 mm	809.1±71.2	786.6±73	777.6±68.5	749.3±61.3	
	5 mm	794.1±83.2	755.8±94.1	750.6±84	725.2±87.9	
Temporal	1 mm	727.3±82.4	760.9±74.5	746.8±85.3	767.8±107	0.6504
	2 mm	698.8±75.6	695.3±50.7	701.9±67.7	702.1±69.8	
	3 mm	736.4±81.5	742.9±66.2	738.1±68.2	749.1±69.5	
	4 mm	751.6±72.1	749.3±76.1	751.3±70.4	761.7±69	
	5 mm	740±78.5	738.7±89	731.6±82.8	750.4±101.3	
Nasal	1 mm	700.3±79.2	685±56	685.9±73.5	708.1±83	0.3308
	2 mm	701±54.4	695.8±58.4	692±62.2	708.7±57.5	
	3 mm	707.5±55.3	700.5±59	704.6±59.1	711.6±68.9	
	4 mm	693.8±55	686.6±69.8	678.8±69	693.8±77.5	
	5 mm	688.6±61	675±75.5	673.1±85.3	674.8±88	

The averaged AST at each of the five latitude lines (i.e., SNIT1, SNIT2, SNIT3, SNIT4, and SNIT5) showed significant variations in myopes compared with emmetropes. Interestingly, the averaged AST is thickest at 3-mm latitude lines in emmetropes, while it is thickest at 1-mm latitude lines in myopes. A previous study demonstrated that AST changes with accommodations at 1 and 3 mm posterior to the scleral spur are more significant in myopes, which can be explained by regional variations in ciliary body thickness and distinct scleral responses to these biomechanical forces between emmetropes and myopes [21]. This finding suggests that the averaged AST at latitude lines, especially at 1- and 3-mm locations, can vary in emmetropes and myopes. The AST along the nasal, temporal, and superior meridians exhibited no significant differences in emmetropes and myopes in our study, which accords with other studies [9,11,12]. In contrast, significant changes were observed along the inferior meridian. Dhakal et al. reported significantly thinner AST in the eyes of myopes compared to emmetropes along the inferior meridian [13], which is consistent with our study. Meanwhile, Dhakal et al. further observed marked changes from the scleral spur to 3-mm locations, while notable changes were found at the 4- and 5-mm locations in the current study. This divergence could be because of the range of myopes (≤ -27.25 D in Dhakal et al.'s study versus ≤ -12.25 D in this study), the different measuring methods (axial AST in Dhakal et al.'s study versus vertical AST in this study), and the addition of ethnicity (Indian in Dhakal et al.'s study versus Chinese in this study). With an increased degree of myopia, AST undergoes thinning only along the inferior meridian, which may be associated with anatomic asymmetry in the orbit. The interspace between the orbital walls and the equatorial plane of the eyeball along the inferior region is greater than that in the other three regions, which allows more interspace to expand for the eyeball. Stephan et al. demonstrated that the distance from the equatorial surface of the eyeball to the inferior orbital margin was greatest (7.8 mm in the inferior) by dissecting adult human cadavers [22]. Atchison et al. also found that in the vertical meridian, the space was greater than that of the horizontal meridian, based on the results of MRIs of emmetropia and myopia [23].

An increasing number of studies have suggested that composition and structure changes in the sclera have been found in experimental animals and in human myopia [24–27]. These tissue-level changes do not mean accelerated scleral growth. Instead, another distinct mechanism underlies myopia: scleral remodeling, which involves the rearrangement of existing material. Collagen metabolism is a critical

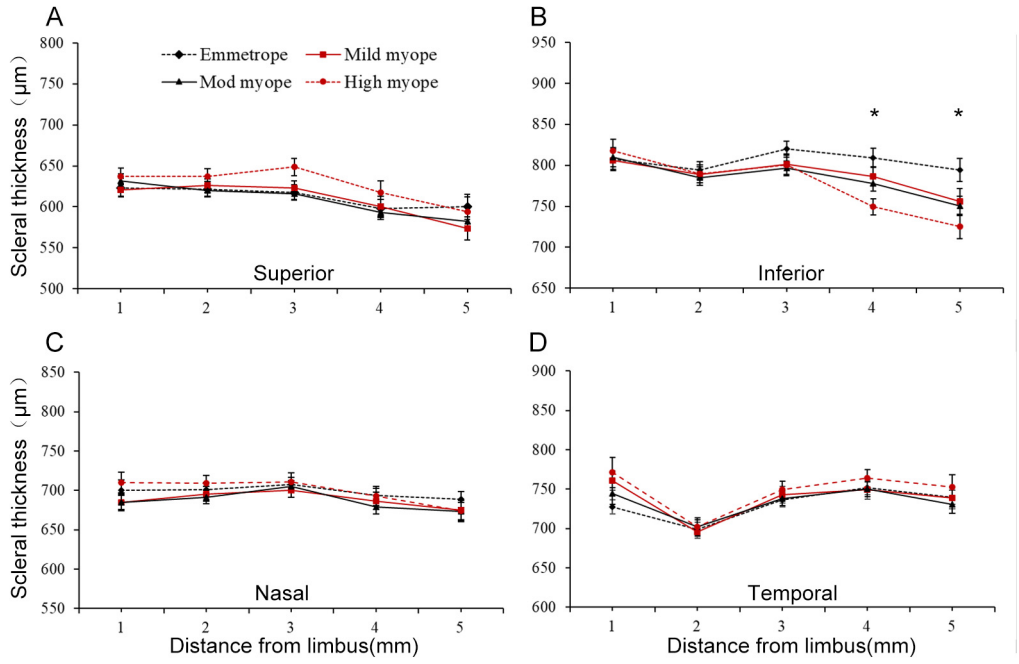

Figure 3. AST with SER errors along four meridians (superior, inferior, nasal, and temporal). "1" indicates the scleral spur to the 1-mm location. "*" represents statistical significance in SER errors. At i4, the mean scleral thickness in the orthopedic group was higher than in the severe myopia group (p = 0.006, adjusted by DUNNETT), and the same trend was observed at i5 (p = 0.0031, adjusted by DUNNETT).

factor in scleral remodeling. Curtin et al. found a reduction in collagen fibril diameter in humans with high myopia [28,29]. We speculate that asymmetries in scleral remodeling could be another potential effect. In addition, the excitation/inhibition of receptors (GABA and muscarinic) on the sclera has been investigated [30,31]. The asymmetric distribution of these receptors may exist, which would directly or indirectly influence AST in myopia. The exact mechanism by which AST in the inferior meridian undergoes thinning with heightening myopia is unclear. Further research is necessary on possible asymmetric scleral remodeling and receptor distribution.

An advantage of this study is the modified measurement approach, which Imanaga used to study scleral thickness (a vertical thickness metric) in central serous chorioretinopathy [17]. In addition, second-generation SS AS OCT with better scanning performance was used to obtain more accurate results. The relatively narrow range of SER errors is a limitation of the current study. Future studies that enroll a wider range of SER errors, especially participants with high myopia (> -12.25 D) would facilitate the research. However, in the process of acquiring images, fixation losses might have occurred and changed the imaged locations. Therefore, further studies are needed to reduce the impact of such biases.

In conclusion, compared with the other three meridians, the inferior meridian (4- and 5-mm posterior to the scleral spur) with an increasing degree of myopia illustrated significant thinning. These findings may indicate that AST plays a significant role in the progression of myopia, particularly in the inferior meridian. To verify this hypothesis, further longitudinal studies are needed to compare scleral thicknesses in stable and progressing myopes across sex, age, and ethnicity groups.

APPENDIX 1. AST FOR EACH OF THE 4 MERIDIANS INDIVIDUALLY.

To access the data, click or select the words "Appendix 1." Mean AST ± standard deviation for each meridian from 1 to 5mm anterior-posterior distances from SS.

APPENDIX 2. THE SCHEMATIC DIAGRAM OF LATITUDE LINES.

To access the data, click or select the words "Appendix 2."

APPENDIX 3. SUPPLEMENTAL TABLE 1.

To access the data, click or select the words "Appendix 3."

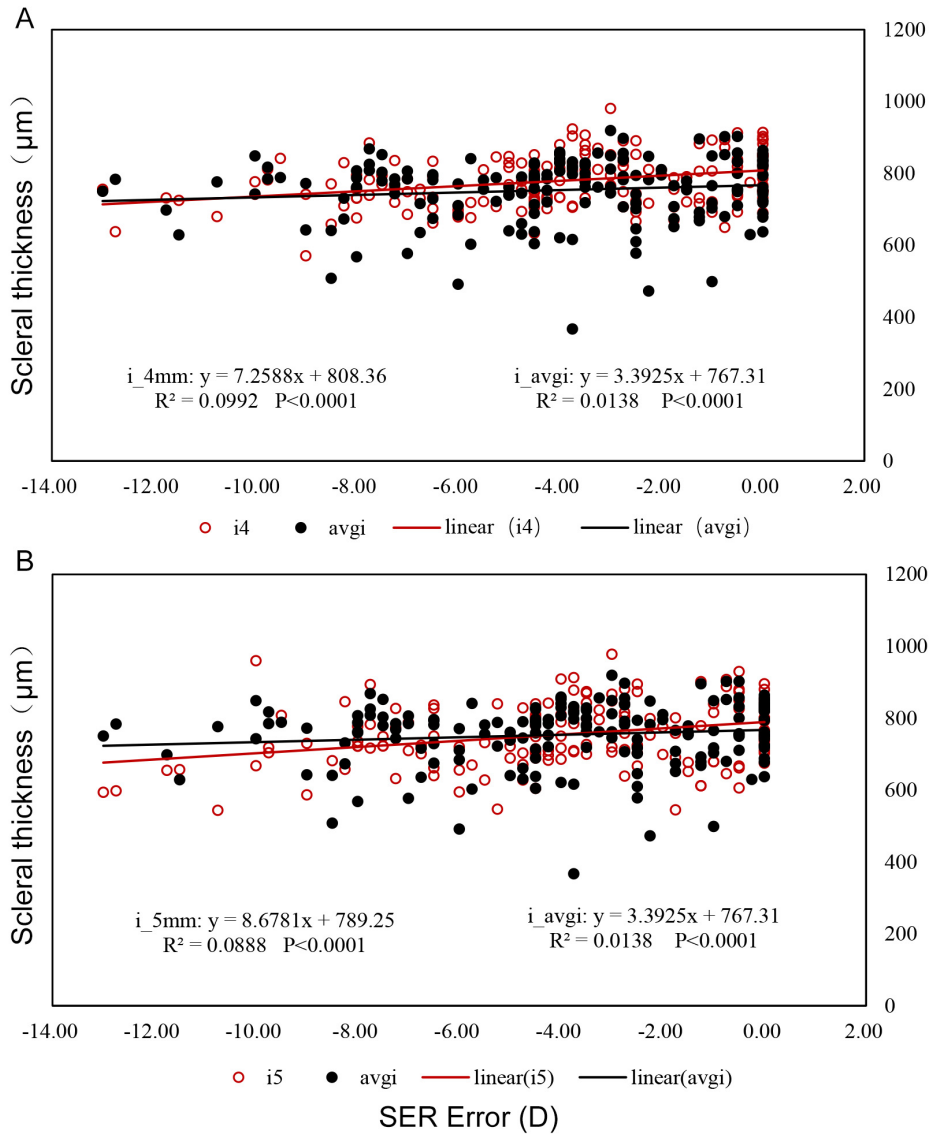

Figure 4. Scatterplots illustrating the relationship between AST and SER errors in the inferior meridian. **A**: Linear regression between the SER error with the AST at the 4-mm location (red empty circle) and averaged peripheral AST (black-filled circles). **B**: Linear regression between an SER error with the AST at the 5-mm location (red empty circle) and averaged peripheral AST (black-filled circles). The linear regression equation results of AST at the 4-mm and 5-mm locations are displayed in the graph. Each scatterplot contained 170 image data from 170 patients.

ACKNOWLEDGMENTS

Disclosure statement: The authors have no conflicts of interest to declare. We would like to thank Huangguo Xiong for his help with the statistical analysis. Author Contributions LZL, QX and MK conceived and designed the study. SCC, YF, YTL and QX collected and measured the data. LZL, QX and SCC analyzed the data and wrote the initial manuscript draft. XMC and LY gave constructive advices about the study. MK and LZL actively reviewed and approved the manuscript.

REFERENCES

1. Holden BA, Fricke TR, Wilson DA, Jong M, Naidoo KS, Sankaridurg P, Wong TY, Naduvilath TJ, Resnikoff S. Global Prevalence of Myopia and High Myopia and Temporal Trends from 2000 through 2050. Ophthalmology 2016; 123:1036-42. [PMID: 26875007].

2. Flitcroft DI. The complex interactions of retinal, optical and environmental factors in myopia aetiology. Prog Retin Eye Res 2012; 31:622-60. [PMID: 22772022].

3. Morgan IG, Ohno-Matsui K, Saw SM. Myopia. Lancet 2012; 379:1739-48. [PMID: 22559900].

4. Vurgese S, Panda-Jonas S, Jonas JB. Scleral thickness in human eyes. PLoS One 2012; 7:e29692[PMID: 22238635].

5. Lin X, Wang BJ, Wang YC, Chu RY, Dai JH, Zhou XT, Qu XM, Liu H, Zhou H. Scleral ultrastructure and biomechanical changes in rabbits after negative lens application. Int J Ophthalmol 2018; 11:354-62. [PMID: 29600166].

6. McBrien NA, Cornell LM, Gentle A. Structural and ultrastructural changes to the sclera in a mammalian model of high myopia. Invest Ophthalmol Vis Sci 2001; 42:2179-87. [PMID: 11527928].

7. Norton TT, Rada JA. Reduced extracellular matrix in mammalian sclera with induced myopia. Vision Res 1995; 35:1271-81. [PMID: 7610587].

8. Rada JA, Achen VR, Penugonda S, Schmidt RW, Mount BA. Proteoglycan composition in the human sclera during growth and aging. Invest Ophthalmol Vis Sci 2000; 41:1639-48. [PMID: 10845580].

9. Buckhurst HD, Gilmartin B, Cubbidge RP, Logan NS. Measurement of scleral thickness in humans using anterior segment optical coherent tomography. PLoS One 2015; 10:e0132902[PMID: 26218188].

10. Ebneter A, Häner NU, Zinkernagel MS. Metrics of the normal anterior sclera: imaging with optical coherence tomography. Graefes Arch Clin Exp Ophthalmol 2015; 253:1575-80. [PMID: 26067393].

11. Read SA, Alonso-Caneiro D, Vincent SJ, Bremner A, Fothergill A, Ismail B, McGraw R, Quirk CJ, Wrigley E. Anterior eye tissue morphology: Scleral and conjunctival thickness in children and young adults. Sci Rep 2016; 6:33796-[PMID: 27646956].

12. Pekel G, Yağcı R, Acer S, Ongun GT, Çetin EN, Simavlı H. Comparison of corneal layers and anterior sclera in emmetropic and myopic eyes. Cornea 2015; 34:786-90. [PMID: 25811725].

13. Dhakal R, Vupparaboina KK, Verkicharla PK. Anterior sclera undergoes thinning with increasing degree of myopia. Invest Ophthalmol Vis Sci 2020; 61:6-[PMID: 32271887].

14. Fukuda S, Ueno Y, Fujita A, Mori H, Tasaki K, Murakami T, Beheregaray S, Oshika T. Comparison of anterior segment and lens biometric measurements in patients with cataract. Graefes Arch Clin Exp Ophthalmol 2020; 258:137-46. [PMID: 31631237].

15. Alonso-Caneiro D, Vincent SJ, Collins MJ. Morphological changes in the conjunctiva, episclera and sclera following short-term miniscleral contact lens wear in rigid lens neophytes. Cont Lens Anterior Eye 2016; 39:53-61. [PMID: 26189941].

16. Read SA, Alonso-Caneiro D, Free KA, Labuc-Spoors E, Leigh JK, Quirk CJ, Yang ZY, Vincent SJ. Diurnal variation of anterior scleral and conjunctival thickness. Ophthalmic Physiol Opt 2016; 36:279-89. [PMID: 26931410].

17. Imanaga N, Terao N, Nakamine S, Tamashiro T, Wakugawa S, Sawaguchi K, Koizumi H. Scleral thickness in central serous chorioretinopathy. Ophthalmol Retina 2021; 5:285-91. [PMID: 32683110].

18. Shen L, You QS, Xu X, Gao F, Zhang Z, Li B, Jonas JB. Scleral and choroidal thickness in secondary high axial myopia. Retina 2016; 36:1579-85. [PMID: 26735565].

19. Norman RE, Flanagan JG, Rausch SM, Sigal IA, Tertinegg I, Eilaghi A, Portnoy S, Sled JG, Ethier CR. Dimensions of the human sclera: Thickness measurement and regional changes with axial length. Exp Eye Res 2010; 90:277-84. [PMID: 19900442].

20. Verkicharla PK, Suheimat M, Schmid KL, Atchison DA. Differences in retinal shape between East Asian and Caucasian eyes. Ophthalmic Physiol Opt 2017; 37:275-83. [PMID: 28370187].

21. Woodman-Pieterse EC, Read SA, Collins MJ, Alonso-Caneiro D. Anterior scleral thickness changes with accommodation in myopes and emmetropes. Exp Eye Res 2018; 177:96-103. [PMID: 30040950].

22. Stephan CN, Davidson PL. The placement of the human eyeball and canthi in craniofacial identification. J Forensic Sci 2008; 53:612-9. [PMID: 18471206].

23. Atchison DA, Jones CE, Schmid KL, Pritchard N, Pope JM, Strugnell WE, Riley RA. Eye shape in emmetropia and myopia. Invest Ophthalmol Vis Sci 2004; 45:3380-6. [PMID: 15452039].

24. Guo L, Frost MR, He L, Siegwart JT Jr, Norton TT. Gene expression signatures in tree shrew sclera in response to three myopiagenic conditions. Invest Ophthalmol Vis Sci 2013; 54:6806-19. [PMID: 24045991].

25. Shen L, You QS, Xu X, Gao F, Zhang Z, Li B, Jonas JB. Scleral and choroidal volume in relation to axial length in infants with retinoblastoma versus adults with malignant melanomas or end-stage glaucoma. Graefes Arch Clin Exp Ophthalmol 2016; 254:1779-86. [PMID: 27116210].

26. Jonas JB, Holbach L, Panda-Jonas S. Scleral cross section area and volume and axial length. PLoS One 2014; 9:e93551[PMID: 24681550].

27. Moring AG, Baker JR, Norton TT. Modulation of glycosaminoglycan levels in tree shrew sclera during lens-induced myopia development and recovery. Invest Ophthalmol Vis Sci 2007; 48:2947-56. [PMID: 17591859].

28. Curtin BJ, Iwamoto T, Renaldo DP. Normal and staphylomatous sclera of high myopia. An electron microscopic study. Arch Ophthalmol 1979; 97:912-5. [PMID: 444126].

29. Ouyang X, Han Y, Xie Y, Wu Y, Guo S, Cheng M, Wang G. The collagen metabolism affects the scleral mechanical properties in the different processes of scleral remodeling. Biomed Pharmacother 2019; 118:109294[PMID: 31404770].

30. Stone RA, Liu J, Sugimoto R, Capehart C, Zhu X, Pendrak K. GABA, experimental myopia, and ocular growth in chick. Invest Ophthalmol Vis Sci 2003; 44:3933-46. [PMID: 12939312].

31. Barathi VA, Weon SR, Beuerman RW. Expression of muscarinic receptors in human and mouse sclera and their role in the regulation of scleral fibroblasts proliferation. Mol Vis 2009; 15:1277-93. [PMID: 19578554].

Articles are provided courtesy of Emory University and the Zhongshan Ophthalmic Center, Sun Yat-sen University, P.R. China. The print version of this article was created on 22 April 2024. This reflects all typographical corrections and errata to the article through that date. Details of any changes may be found in the online version of the article.